Hole-polaron formation in the two-dimensional Holstein t-J model: A variational Lanczos study

H. Fehske, H. Röder, and G. Wellein
Physikalisches Institut, Universität Bayreuth, D-95440 Bayreuth, Germany

A. Mistriotis
Research Centre of Crete, P.O. Box 1527, Heraklio 71110, Crete, Greece
(Received 17 February 1995)

Polaronic features of dopant-induced charge carriers are manifest in recent experiments on $La_{2-x}Sr_xCuO_{4+y}$ and $La_{2-x}Ni_xCuO_{4+y}$. To study the formation of hole (bi)polarons in such systems exhibiting strong Coulomb interactions, the Holstein t-J model is examined by means of a variational diagonalization technqiue for a wide range of phonon frequencies and electron-phonon (EP) couplings on finite square lattices, up to 18 effective sites in size. Including static displacement field, polaron, and squeezing effects, our approach allows for the description of nearly free polarons in the weak-coupling limit as well as for adiabatic Holstein polarons and nonadiabatic Lang-Firsov polarons in the case of strong EP interactions. At low doping levels and low phonon frequencies we demonstrate that antiferromagnetic spin correlations and EP interactions reinforce each other to the effect of lowering the threshold for polaronic self-localization in a strongly distorted lattice. This is contrasted with the nonadiabatic regime, where we observe the formation of Lang-Firsov polarons with moderate polaronic mass enhancement in a nearly undistorted lattice. In the case of two doped holes, the hole binding energy is analyzed in detail and we find that hole binding is enhanced as a dynamical (static) effect of a rather weak (extremely strong) EP interaction for delocalized (self-trapped) polarons. At quarter-filling we notice, in the adiabatic regime, a sequence of transitions as the EP coupling increases from nearly free mobile polarons to a polaronic superlattice and finally to a charge-separated state. The ordering of polarons disappears at higher phonon frequencies.

I. INTRODUCTION

Although no definite conclusion can be drawn so far whether the electron-phonon (EP) coupling is responsible for the pairing interaction in the high-T_c superconductors, there is, however, growing consensus that the lattice degrees of freedom are essential in understanding the puzzling normal-state properties of the high-T_c compounds. In particular, the relevance of EP coupling can be seen from the experimental observation of phonon renormalization in the cuprates.[1] An important question to be answered is whether the dopant-induced charge caries, moving in the strongly antiferromagnetic correlated Cu^{2+}-spin background of the CuO_2 planes, exhibit a significant phonon dressing. In the presence of strong Coulomb correlations, a rather weak EP interaction already can cause polaronic band narrowing[2] and might, therefore, drive the system further into the strongly correlated regime. In the normal state of the metallic cuprates, there is indeed experimental evidence for polaronic effects,[3,4] as well as for large anharmonic lattice vibrations which could be taken as an ingredient of polaron formation, like for example, the apical breathing mode in $YBa_2Cu_3O_{7-\delta}$.[5]

From a theoretical point of view, the nature of the so-called self-trapping transition, which describes the transformation of a band of quasi-free charge carriers to one of heavily dressed polaronic quasiparticles is one of the most challenging problems in strongly coupled EP systems. Since Landau's early suggestion of a delocalization-localization transition in 1933 (Ref. 6) numerous work has been performed to tackle the formation of bipolarons/polarons (see Refs. 7–10 for recent reviews). However, we still lack a complete understanding of this transition and even of the basic features of the polaronic or bipolaronic state (cf. the heated debates concerning the question of whether small bipolarons/polarons can move itinerantly[4]). Especially for the multielectron system and in the regime of intermediate EP coupling, there are up to now no well-controlled analytical techniques to analyze the polaron problem. These difficulties have led several groups to investigate the polaronic properties of small clusters using numerical techniques. In diagonalization methods, the infinite phononic Hilbert space has to be truncated, which limits the accessible parameter regime in accordance with the maximum dimension of the matrices one can tackle. Ranninger and Thibblin[11] give a complete numerical solution of the two-site Holstein-Hubbard model. In a recent calculation by Marsiglio[12] the weak-coupling regime (with few phonons) was investigated. Independent exact diagonalizations of the 1D and 2D Holstein-Hubbard model have been performed by Aleksandrov *et al.*[13] and Wellein *et al.*[14,15] in the small electron density limit for a wider range of the EP coupling including the transition regime. In spite of these advantages, memory limitations impose severe restrictions on the phononic Hilbert space truncation method, which becomes difficult in the low-

0163-1829/95/51(23)/16582(12)/$06.00

frequency strong-coupling regime, where a large number of phonon states is required.

In order to obtain results for higher electron densities and to access the complete range of phonon frequencies and EP couplings, in this work we present a numerical diagonalization scheme based on an inhomogeneous modified variational Lang-Firsov transformation. We use this technique to study the interplay between the EP coupling and the strong electron-electron interaction in terms of the probably most simple microscopic model suitable for a description of EP effects in the high-T_c cuprates; the two-dimensional Holstein t-J model. The paper is organized as follows. In Sec. II, we introduce the Holstein t-J model and outline the variational Lanczos approach. The ground-state properties of the resulting effective polaronic t-J model are examined on finite lattices up to 18 sites in Sec. III. To investigate the quality of the variational Lanczos method, we compare it with numerical exact results for the Holstein-Hubbard model in Sec. IV. We summarize in Sec. V.

II. MODEL AND METHODOLOGY

The Hamiltonian of the Holstein t-J model is given by

$$\begin{aligned}\mathcal{H}_{H-t-J} = & -t \sum_{\langle ij\rangle\sigma} (\tilde{c}_{i\sigma}^{\dagger}\tilde{c}_{j\sigma} + \text{H.c.}) \\ & + J \sum_{\langle ij\rangle} (\mathbf{S}_i\mathbf{S}_j - \tfrac{1}{4}\tilde{n}_i\tilde{n}_j) \\ & - \sqrt{\varepsilon_p \hbar\omega} \sum_i (b_i^{\dagger} + b_i)\tilde{h}_i + \hbar\omega \sum_i (b_i^{\dagger}b_i + \tfrac{1}{2}) \, .\end{aligned} \tag{1}$$

$\mathcal{H}_{H-t-J}$ acts in a projected Hilbert space without double occupancy, where $\tilde{c}_{i\sigma}^{(\dagger)} = c_{i\sigma}^{(\dagger)}(1-\tilde{n}_{i\bar{\sigma}})$ is the electron annihilation (creation) operator, $\tilde{n}_i = \Sigma_\sigma \tilde{c}_{i\sigma}^{\dagger}\tilde{c}_{i\sigma}$, and $\mathbf{S}_i = \frac{1}{2}\Sigma_{\sigma\sigma'}\tilde{c}_{i\sigma}^{\dagger}\tau_{\sigma\sigma'}\tilde{c}_{i\sigma'}$. $\tilde{h}_i = 1 - \tilde{n}_i$ denotes the hole number operator. The first two terms represent the standard t-J model, where J measures the antiferromagnetic exchange interaction and t denotes hopping processes between nearest-neighbor pairs $\langle ij\rangle$ on a square lattice. The third and fourth terms take the EP interaction and the phonon energy in a harmonic approximation into account. Here, ε_p is the EP coupling constant, ω the bare phonon frequency, and $b_i^{(\dagger)}$ are the phonon annihilation (creation) operators. In the context of an effective single-band description of the copper/nickel oxides, the dominant source of EP coupling is assumed to come from the interaction of doped holes with a single dispersionless phonon mode.[16] Then the collective Holstein-coordinates $q_i = \sqrt{\hbar/2M\omega}(b_i^{\dagger} + b_i)$ may be thought of as representing *local* apical out-off plane or bond-parallel in-plane breathing-type displacements of oxygen atoms, i.e., the q_i can be interpreted as an internal optical degree of freedom of the lattice site i. The physics of the Holstein t-J model is governed by three competing effects: the itinerancy (t) of doped charge carriés (holes), their strong Coulomb correlations (due to J/t and the constraint of no double occupancy), and the polaronic band renormalization, due to the local Holstein-type hole-phonon interaction ($\varepsilon_p/t, \hbar\omega/t$).

Concerning the EP part, the condition $\varepsilon_p/t \ll 1$ ($\gg 1$) refers to the weak- (strong-) coupling regime, whereas for $\sqrt{\varepsilon_p/\hbar\omega} \ll 1$ ($\gg 1$), single-phonon (multiphonon) processes are involved in the electron dynamics.[17] In the single-electron case, the Holstein Hamiltonian has been studied extensively as a paradigmatic model for polaron formation.[8,18] The principal result is that the effective mass of a single charge carrier coupled strongly to the local lattice vibrations becomes very heavy, making the particle susceptible to self-trapping. Monte Carlo simulations[19] indicate that the transition from a wide-band Fermi liquid to narrow-band polaronic system is *continuous* but *rather sharp* and takes place in the intermediate region of EP coupling. Note that the Migdal theorem is violated under this familiar polaronic band collapse driven by the instability of the phonon vacuum.[8] Whereas the weak-coupling regime is well understood and dealt with by perturbation theory and variational techniques, there are, depending on the ratio $\hbar\omega/t$, two completely different types of approximations in the strong-coupling region.[10] The first approach, based on the Lang-Firsov canonical transformation[20] followed by the zero-phonon approximation, yields exact results in the antiadiabatic limit $\hbar\omega \gg t$. It describes the case of small (nonadiabatic) Lang-Firsov polarons. The second approach is based on an expansion in $\hbar\omega/t$, which has been worked out by Holstein[21] for the two-site model only and yield another type of (heavy) polarons, the so-called adiabatic Holstein polarons. Note that in the adiabatic limit $\hbar\omega \ll t$, the procedure of averaging over phonons to obtain the renormalized polaronic bandwidth is incorrect.[13] Recently Kabanov and Mashtakov[22] have obtained the main results of the adiabatic approach from a functional integral method, which takes the extremal displacement field configurations into account. We would like to emphasize that the situation becomes much less clear if the energy scales are not well separated, e.g., in the intermediate regime $\varepsilon_p \sim \hbar\omega \sim t$. Furthermore, for the multielectron systems, collective phenomena become important, which may result in a variety of phases as a function of band filling and interaction strengths including, e.g., (incommensurate) charge- and spin-density-wave, bipolaronic or superconducting ground states.

In what follows, we present a variational Lanczos approach that allows for the description of the aforementioned limiting cases, with respect to the EP coupling and includes exactly the strong Coulomb correlations. As a first step, we perform an inhomogeneous modified variational Lang-Firsov (IMVLF) transformation,

$$\tilde{\mathcal{H}}_{H-t-J} = \mathcal{U}^{\dagger}\mathcal{H}\mathcal{U} \, , \quad \mathcal{U} = e^{-\mathcal{S}_1(\{\Delta_i\})} e^{-\mathcal{S}_2(\gamma,\bar{\gamma})} \, , \tag{2}$$

with

$$\mathcal{S}_1 = \frac{1}{2\sqrt{\varepsilon_p\hbar\omega}} \sum_i \Delta_i (b_i^{\dagger} - b_i) \, , \tag{3}$$

$$\mathcal{S}_2 = -\sqrt{\varepsilon_p/\hbar\omega} \sum_i (b_i^{\dagger} - b_i)(\bar{\gamma} + \gamma\tilde{h}_i) \, . \tag{4}$$

The first canonical transformation $\mathcal{S}_1(\{\Delta_i\})$ introduces a set of static *site-dependent* displacement fields Δ_i, i.e., there is *a priori* no restriction to a specific type of charge-density wave order, like for example, a frozen-in (π,π) dimerization.[23,24] $\mathcal{S}_1$ is designed to describe static *local* lattice distortions and ensures the correct behavior of our theory in the *adiabatic* limit. To treat the formation of polarons at arbitrary band fillings, a second unitary transformation $\mathcal{S}_2(\gamma,\overline{\gamma})$ was performed, where the variational parameter γ measures the degree of the polaron effect ($0\le\gamma\le 1$), which becomes most important in the low carrier density *antiadiabatic* limit [cf. the results of the standard polaron theories ($\gamma\equiv 1,\overline{\gamma}\equiv 0$) (Ref. 20)]. Next, we construct a variational ground state

$$|\Psi_V\rangle = |\Psi_{\rm ph}\rangle \otimes |\Psi_{\rm el}\rangle \ , \tag{5}$$

where the squeezed two-phonon coherent state[25]

$$|\Psi_{\rm ph}\rangle = \exp\left\{\alpha \sum_i (b_i^\dagger b_i^\dagger - b_i b_i)\right\}|0\rangle \ , \tag{6}$$

allows for the anharmonicity of the lattice fluctuations. The squeezing effect described by a further variational parameter ($\tau^2=\exp\{-4\alpha\}$, $\alpha>0$) should be of special importance at finite-polaron densities and in the *intermediate* coupling and frequency regime.[17,26] Averaging over the transformed phonon vacuum, one obtains the effective polaronic t-J model,

$$\mathcal{H}^{\rm eff}_{H-t-J} = \frac{\hbar\omega}{4} N(\tau^2+\tau^{-2}) + \overline{\gamma}^2\varepsilon_p N + \frac{1}{4\varepsilon_p}\sum_i \Delta_i^2 + \lambda\sum_i \Delta_i$$
$$+ (1-\gamma)\sum_i \Delta_i \tilde{h}_i - \varepsilon_p[2\gamma-\gamma^2+2\overline{\gamma}(1-\gamma)]\sum_i \tilde{h}_i - \rho t \sum_{\langle ij\rangle\sigma} (\tilde{c}^\dagger_{i\sigma}\tilde{c}_{j\sigma} + \text{H.c.}) + J\sum_{\langle ij\rangle}(\mathbf{S}_i\mathbf{S}_j - \tfrac{1}{4}\tilde{n}_i\tilde{n}_j) \ , \tag{7}$$

where

$$\rho = \exp\{-\varepsilon_p\gamma^2\tau^2/\hbar\omega\} \ , \tag{8}$$

and the Lagrange multiplier λ enforces the constraint $\sum_i \Delta_i = 0$. Note that in this approach the dynamic part of the residual polaron-multiphonon interaction is neglected. The adiabatic limit $\hbar\omega\to 0$, however, where $\gamma,\overline{\gamma}\to 0$ and $\rho,\tau^2\to 1$, is correctly reproduced and the Hamiltonian (7) becomes the adiabatic Holstein t-J model recently studied by the authors.[27,28]

In order to investigate the ground-state properties of the polaronic t-J model, we use the Lanczos diagonalization technique in the subspace of fixed hole numbers N_h and minimal total S^z. According to Hellmann-Feynman's theorem, the minimal total energy $E(\gamma,\overline{\gamma},\tau^2,\{\Delta_i\})$ and the associated wave function $|\Psi_{\rm el}(\gamma,\overline{\gamma},\tau^2,\{\Delta_i\})\rangle$ can be obtained by iteratively solving the following set of $2N+4$ self-consistency equations:

$$\overline{\gamma} = (1-\gamma)\delta \ , \quad \lambda = -\overline{\gamma} \ , \tag{9}$$

$$\gamma = \frac{\hbar\omega[\delta(1-\delta)+E_{\Delta h}/2\varepsilon_p]}{\hbar\omega\delta(1-\delta)-\tau^2 E_t} \ , \tag{10}$$

$$\tau^2 = \frac{\hbar\omega}{\sqrt{\hbar^2\omega^2 - 4\varepsilon_p\gamma^2 E_t}} \ , \tag{11}$$

$$\Delta_i = 2\varepsilon_p(1-\gamma)(\delta-\delta_i) \ . \tag{12}$$

Note that each iteration step involves the Lanczos diagonalization of the Hamiltonian (7). Since the free spatial variation of the displacement fields Δ_i, in general, breaks the translation invariance, we have to work with an unsymmetrized basis set of many particle states. In (9)–(12),

$$E_{\Delta h} = \frac{1}{N}\sum_i \langle \Delta_i \tilde{h}_i \rangle \ , \tag{13}$$

$$E_t = -\frac{\rho t}{N}\sum_{\langle ij\rangle\sigma} \langle (\tilde{c}^\dagger_{i\sigma}\tilde{c}_{j\sigma} + \text{H.c.})\rangle \ , \tag{14}$$

and

$$\delta_i = \langle \tilde{h}_i \rangle \ , \quad \delta = \frac{1}{N}\sum_i \delta_i \tag{15}$$

denote the kinetic energy, (static) electron-lattice contribution to the ground-state energy, and the local (mean) hole density $\delta_i(\delta)$, respectively, where $\langle\ \rangle = \langle\Psi_{\rm el}(\gamma,\overline{\gamma},\tau^2,\{\Delta_i\})|\cdots|\Psi_{\rm el}(\gamma,\overline{\gamma},\tau^2,\{\Delta_i\})\rangle$. In addition, we define the averaged displacement field

$$\Delta = \frac{1}{N}\sum_i |\Delta_i| \ , \tag{16}$$

which plays to some extent the role of an order parameter separating (nearly free) delocalized hole states from mainly localized adiabatic Holstein polarons, and as a measure of the phonon-induced band renormalization the effective transfer amplitude

$$t_{\rm eff} = E_t(\varepsilon_p,J)/E_t(0,J) \ . \tag{17}$$

Obviously, $t_{\rm eff}$ differs from the pure polaronic band-narrowing factor ρ.

III. NUMERICAL RESULTS FOR THE 2D HOLSTEIN t-J MODEL

In the numerical work, we proceed as follows. First, we restrict the system size to the ten-site lattice (cf. Fig. 1) in order to investigate the ground-state properties of the model (7) at different band fillings for a wide range of EP coupling strengths and phonon frequencies. The exchange interaction strength is fixed to $J/t=0.4$ (which seems to be a reasonable value with respect to the strong correlations observed in the high T_c's). In a next step, we check that the qualitative results remain unchanged for a few representative parameter values on the 16- and 18-

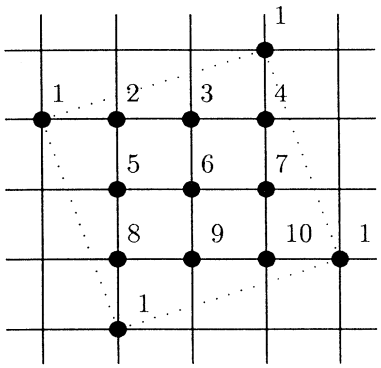

FIG. 1. The tilted effective ten-site lattice used in this work. Periodic boundary conditions are applied at the dotted lines.

site lattice. Note that for the 18-site single-hole system, it takes approximately 60 000 cpu seconds of a Cray Y-MP to get the ground state and the variational parameters with sufficient accuracy (relative error of the ground-state energy 10^{-8}; matrix dimension 437.580). In the following, all the energies are measured in units of t.

A. One- and two-hole case

In the analysis of the polaronic t-J model, we shall start with the study of just a single dynamic hole. Due to the competition between the antiferromagnetic exchange energy lost and the delocalization energy gain this problem is highly nontrivial even for the pure t-J model, and a considerable effort has been devoted to this subject.[29] Including the EP coupling, both static lattice deformations ($\hbar\omega \ll \varepsilon_p, t$) and dynamic polaron formation ($\hbar\omega, \varepsilon_p \gg t$) can introduce anharmonic effects, further enhancing the effective mass of the charge carriers. For a more quantitative discussion, we show in Fig. 2 the effective transfer amplitude t_{eff}, the polaronic band-narrowing factor ρ, and the averaged static displacement Δ as a function of ε_p. For low frequencies ($\hbar\omega < t$), we can distinguish two main regimes, referred to below as nearly free polarons (FP) and adiabatic Holstein polarons (AHP). In the FP state for small $\varepsilon_p \leq 0.4$, the ground state reflects the translational symmetry of the ground state of the pure t-J model,[30] i.e., the hole is mainly delocalized and we observe two hole sites, where the spin density is concentrated (cf. the on-site electron/spin densities tabulated in Table I). In addition, the polaron effect is very weak [cf. the γ value at $\varepsilon_p = 0.2$ given in Table I and ρ vs ε_p shown in the inset of Fig. 2(b)]. Note that for the FP state at $J = 0.4$, the finite (but very small) value of Δ [Fig. 2(b)] is due to the nontrivial wave vector of the electronic part of the ground-state wave function. If we take, for example, $J = 0.1$, where the momentum of the ground state is zero, we found $\langle n_i \rangle = 0.9$ $\forall i$ and $\Delta \equiv 0$ in this regime. Increasing the EP coupling the mobility of the hole ($\propto t_{\text{eff}}$) is strongly reduced and an AHP is formed. As can be seen from Fig. 2(b) and Table I, a strong local static lattice distortion traps the hole mainly on a single site for $\varepsilon_p > \varepsilon_{p,1}^{c} \sim 0.4$. At the same time, we observe a significant enhancement of the antiferromagnetic spin correlations $\langle S_i^z S_j^z \rangle$ between nearest-neighbor sites in the spin background, i.e., the substantial gain in exchange and EP interaction energy overcompensates the cost of elastic and kinetic energy. On the other hand, the polaronic variational parameter γ becomes even smaller, which means that ρ is not influenced by this self-transition transition. This is worth emphasizing because it shows that our IMVLF approach incorporates two different types of polaronic states, the adiabatic Holstein polarons (AHP) and the nonadiabatic Lang-Firsov polarons (NLFP). To discuss the effect of the electronic correlations on the self-trapping transition, we have considered the (noninteracting) case of spinless fermions ($S^z = S^z_{\text{max}}$). For the one-hole case, this can be mimicked by setting $J = 0$ (Nagaoka limit) and is, of course, equivalent to the one-electron Holstein model. Obviously, we obtain the transition at a much larger critical EP interaction $\varepsilon_{p,1}^{c,\text{SF}} \sim 4.0$, which is in the order of half the

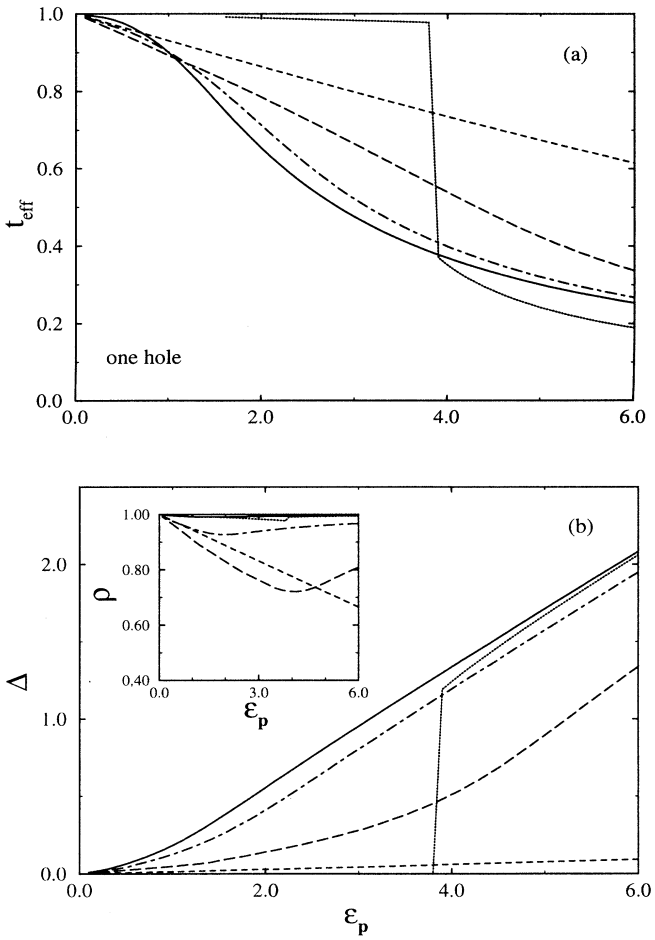

FIG. 2. Dependence of the effective transfer amplitude t_{eff} (a), averaged static displacement Δ (b), and the polaronic band narrowing factor ρ (inset) on the EP coupling ε_p for the one-hole case. The solid, chain-dashed, long-dashed, and dashed curves refer to $\hbar\omega = 0.1$, 0.8, 3.0, 10.0, respectively. At $\hbar\omega = 0.1$, the corresponding dependencies are given for the case of spinless fermions (dotted curves).

TABLE I. Shifted ground-state energy ($E=E_{\rm tot}-N\hbar\omega/2$), polaron ($\gamma$), and squeezing ($\tau^2$) variational parameter, as well as the on-site electron ($\langle n_i\rangle$) and spin ($\langle S_i^z\rangle$) densities for the ground state of the 2D Holstein t-J model at $J=0.4$. The results are given for one and two holes on a ten-site lattice with periodic boundary conditions at characteristic EP coupling strengths (ε_p) and phonon frequencies ($\hbar\omega$). The sites are counted according to Fig. 1, where values that are emboldened indicate hole sites with lower than the averaged electron density (see text). For $N_h=2$, we have $\langle S_i^z\rangle\equiv 0$.

	$N_h=1$			$N_h=2$		
ε_p	0.2	4.0	4.0	0.2	4.0	4.0
$\hbar\omega$	0.8	0.8	10.0	0.8	0.8	10.0
E	−6.070 11	−8.443 94	−9.320 13	−7.5940	−12.1313	−14.0264
γ	0.221 12	0.100 05	0.824 42	0.195 740	0.107 873	0.804 983
τ^2	0.992 60	0.987 81	0.990 20	0.987 539	0.976 541	0.980 293
i	$\langle n_i\rangle/\langle S_i^z\rangle$			$\langle n_i\rangle$		
1	**0.7782/+0.2386**	**0.0712/+0.0169**	**0.7593/+0.2257**	**0.7679**	**0.0644**	**0.7554**
2	0.9304/+0.0028	0.9826/+0.2300	0.9352/+0.0061	**0.7679**	**0.0644**	**0.7554**
3	0.9304/+0.0028	0.9996/−0.1608	0.9352/+0.0061	0.8214	0.9787	0.8300
4	0.9304/+0.0028	0.9826/+0.2300	0.9352/+0.0061	0.8214	0.9787	0.8300
5	0.9304/+0.0028	0.9996/−0.1608	0.9352/+0.0061	0.8214	0.9787	0.8300
6	**0.7782/+0.2386**	0.9999/+0.2065	**0.7593/+0.2257**	**0.7679**	0.9995	**0.7554**
7	0.9304/+0.0028	0.9996/−0.1608	0.9352/+0.0061	**0.7679**	0.9995	**0.7554**
8	0.9304/+0.0028	0.9826/+0.2300	0.9352/+0.0061	0.8214	0.9787	0.8300
9	0.9304/+0.0028	0.9996/−0.1608	0.9352/+0.0061	0.8214	0.9787	0.8300
10	0.9304/+0.0028	0.9828/+0.2300	0.9352/+0.0061	0.8214	0.9787	0.8300

bare bandwidth. Due to the strong coupling of spin and hole dynamics in the t-J model, the characteristic energy scale for the single-hole motion is J and not t; therefore, we get $\varepsilon_{p,1}^c\sim J=0.4$. Increasing $\hbar\omega$ in the adiabatic regime the transition from FP to AHP is shifted to somewhat larger values of ε_p. For high phonon frequencies ($\hbar\omega\gg t$), we found a smooth crossover from light FP to NLFP, whereby the effective mass ($t_{\rm eff}$) becomes enhanced. In contrast to the adiabatic regime, the mass enhancement now results from the dynamical polaronic band renormalization $\propto\rho$, i.e., $\gamma\to 1$ [see Fig. 2(b) and Table I]. On the other hand, the static lattice distortions almost disappear and the $\langle n_i\rangle$ exhibit the same spatial variation as for the pure t-J model (cf. Table I). Let us emphasize that the polaronic mass renormalization is rather moderate and vanishes in the antiadiabatic limit $\hbar\omega>\varepsilon_p\gg t$, where the polaron effect becomes strongest ($\gamma=1$). Indeed, increasing ε_p further at large but fixed $\hbar\omega$, we always obtain a transition to the self-trapped AHP state. That means, within our IMVLF-Lanczos treatment, we found no parameter region where an extremely heavy NLFP ($\rho\to 0$) does exist. This fact seems to be in agreement with the exact results presented in Sec. IV for the single-electron Holstein model.

Now, let us consider the two-hole case. Here, at $\varepsilon_p=0$ (pure t-J model), the ground state has $S=0$ and a momentum being one of the star of $\mathbf{k}=(0,0)$, $(2\pi/5,4\pi/5)$ for $J\geq 0.201$ or $\mathbf{k}=(0,0)$ for $J<0.201$. At finite EP coupling, $t_{\rm eff}$, ρ and Δ, depicted in Fig. 3 as a function of ε_p, show qualitatively the same behavior as for the one-hole case. Depending on the EP coupling strength, the holes will be trapped in the adiabatic regime, for large enough ε_p, on two adjacent sites sharing the same lattice distortion (cf. Table I). In the context of the Holstein t-J model (double occupancy is strictly forbidden), this can be interpreted as a formation of an adiabatic Holstein bipolaron. Compared to the one-hole case, the transition from FP to the self-trapped state takes place at large critical coupling ($\varepsilon_{p,2}^c\sim 2\varepsilon_{p,1}^c$), which can be traced back to a larger effective transfer amplitude of the pure t-J model with two holes [$E_{t,2}(J,\varepsilon_p=0)=-0.536\sim 2E_{t,1}(J,\varepsilon_p=0)=-0.249$] at $J=0.4$. Of special interest is the question whether the EP interaction enhances the two-hole binding energy, defined as usual by $E_B^2(J,\varepsilon_p,\hbar\omega)=E_2+E_0-2E_1$ (the lower indices denote the hole numbers). If two holes minimize their energy by producing a bound state, then E_B^2 becomes negative. In Table II, the binding energies of two holes are given with respect to the Heisenberg antiferromagnetic state at half-filling ($N_h=0$). At $\varepsilon_p=0$, it is clear that a bound state of holes will be formed at large values of J since two holes on neighboring sites lose the exchange energy on only seven bonds together instead of on eight bonds. Contrary, at very small J, one would expect two independent holes (note that a hole repulsion $E_B^2>0$ obtained from a finite-cluster calculation should vanish in the bulk limit). To exclude finite-size effects in calculating E_B^2 at finite ε_p, one has to take care that one compares the same type of ground state for the one- and two-hole systems, respectively. In the FP regime (see Table II, $\varepsilon_p=0.1$, 0.2 at $J=0.4$), hole binding is enhanced as ε_p increases, whereas at fixed ε_p, it slightly decreases with increasing phonon frequency. This behavior is a net result, including both the static and the dynamic effect of the EP coupling. As mentioned above, due to the nontrivial symmetry of the electronic wave

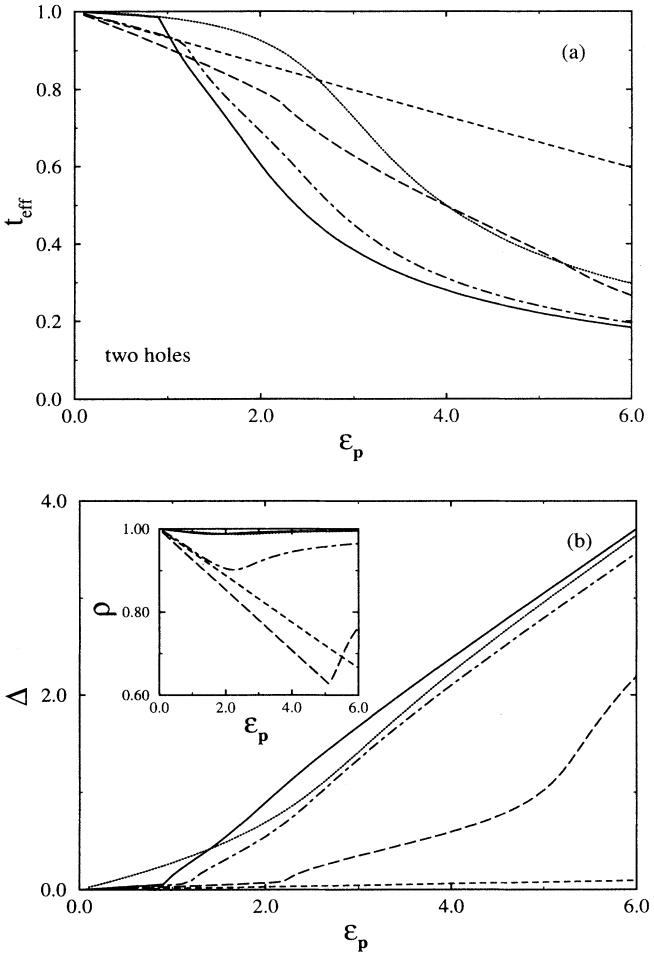

FIG. 3. t_{eff} (a), Δ (b), and ρ (inset) vs ε_p for the two-hole case. The notations are the same as in Fig. 2.

function, the ground-state carries a small but finite static distortion even in the FP state, which becomes enhanced $\propto \varepsilon_p$. Then the effect of a finite-phonon frequency is twofold. First, it counteracts such an enhancement of the static displacement fields and therefore weakens the static part of the binding energy E_B^2. On the other hand, we have found convincing numerical evidence that in the FP state hole attraction may result as a purely dynamic effect of the EP coupling. To show this, it is instructive to calculate E_B^2 at $J=0.1$, where the one- and two-hole FP ground state is uniform [$\mathbf{k}=(0,0)$] up to $\varepsilon_p \lesssim 3.0$, i.e., $\Delta \equiv 0$. In this case, $E_B^2(>0)$ is strongly reduced with increasing ε_p (see Table II). In addition, we observe that now the strongest attraction of hole polarons results for an *intermediate* phonon frequency, where $\hbar\omega$ and the renormalized transfer amplitude are about equal in value. For example, at $\varepsilon_p=2.5$ and $\hbar\omega=0.8$, we have $t_{\text{eff},1}=\rho_1 \sim t_{\text{eff},2}=\rho_2 \sim 0.9$ (remember that $\rho \to 1$ if $\hbar\omega \to 0, \infty$). To complete the analysis of hole binding, let us turn to the adiabatic strong EP coupling regime. In the limit $\varepsilon_p \gg (\hbar\omega, t)$, the two AHP become self-trapped on nearest-neighbor sites forming a nearly immobile bipolaron (cf. Table II). As one increases the phonon frequency, one observes a weaker localization effect. As Table II shows, our expectation of finding a negative binding energy at extremely large coupling, like $\varepsilon_p=10.0$, is correct. However, it is important to note that this static type of hole binding, forced by both ε_p and J (the spin background becomes a nearly perfect antiferromagnet in this case), is much less effective than the dynamic one in the weak-coupling (FP) regime.

Finally, to check for finite-size effects in the results presented above, t_{eff} was calculated on square lattices with 16 and 18 sites. For the particular case of a single hole, results are shown in Fig. 4 at $\hbar\omega=0.1$ and $\hbar\omega=10.0$, corresponding to adiabatic and antiadiabatic regimes. As is intuitively clear, we find the finite-size dependence to be weaker than that in the antiadiabatic limit. But also in the adiabatic region, no major differences between the currently available cluster sizes are observed. Especially, the qualitative features of the weak-coupling FP and strong-coupling AHP states remains unchanged. Note that with increasing lattice size, the AHP becomes even more localized for $\varepsilon_p \gg t \gg \hbar\omega$.

B. Quarter-filled band case

The strongest evidence for polaron formation in doped charge-transfer oxides is provided by recent experiments on $La_{2-x}Sr_xNiO_4$.[3,31] As pointed out by Anisimov *et al.*,[32] the big difference from the isostructural cuprates is the much stronger magnetic confinement effect of additional holes and nickel spins. These low-spin composite holes are nearly entirely prelocalized and the EP coupling becomes much more effective in causing polarons. As a

TABLE II. Binding energy E_B^2 of two holes in the ground state of the Hamiltonian (7) at different exchange interactions J, EP couplings ε_p, and phonon frequencies $\hbar\omega$.

$\hbar\omega$	E_B^2							
	$J=0.4$				$J=0.1$		$J=0.0$	
	$\varepsilon_p=0.0$	0.1	0.2	10.0	$\varepsilon_p=0.0$	2.5	$\varepsilon_p=0.0$	2.5
0.0	−0.3609	−0.3744	−0.3877	−0.2755	+0.5198	+0.0198	+2.0000	+1.5000
0.1		−0.3732	−0.3853	−0.2751		+0.0065		+1.4868
0.4		−0.3703	−0.3794	−0.2738		−0.0208		+1.4597
0.8		−0.3680	−0.3738	−0.2720		−0.0354		+1.4453
1.2		−0.3654	−0.3694	−0.2701		−0.0345		+1.4463
3.0		−0.3616	−0.3613	−0.2601		+0.0315		+1.5125

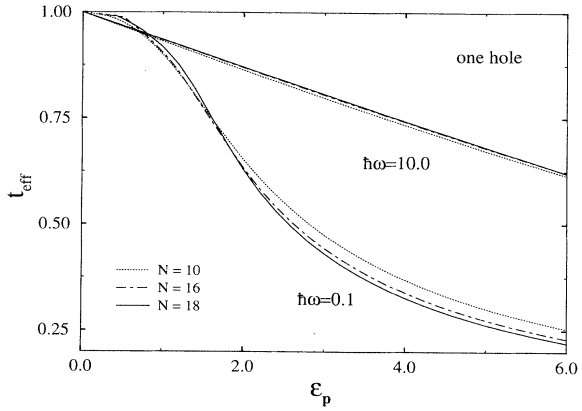

FIG. 4. Effective hopping amplitude $t_{\rm eff}$ vs ε_p for the 2D Holstein t-J model with a single hole. Results are given for lattices with $N=10$, 16, and 18 sites in the adiabatic ($\hbar\omega=0.1$; lower curves) and antiadiabatic ($\hbar\omega=10.0$; upper curves) regimes.

result a complex variety of (incommensurate) charge- and spin-ordering phenomena, related to magnetic and transport anomalies, have recently been observed at low doping ($x\approx 1/3$).[31,33,34] For the composition $La_{1.5}Sr_{0.5}NiO_4$ (quarter filling, $x=0.5$), the electron-diffraction measurements show a commensurate superstructure spot at the (π,π) point, which is interpreted as truly 2D ordering of breathing-type polarons, i.e., as a polaronic superlattice. Since for a theoretical description of the nickelates both the electronic and lattice degrees of freedom are of fundamental importance, the simplest models are then of the Peierls-Hubbard variety. Along this line multiband models, accounting for the more complex high-spin low-spin coupling in the nickelates, were proposed and studied within (unrestricted) Hartree-Fock approximation.[35,36]

Here, we investigate the more simple Holstein t-J model at quarter filling and show that interplay of charge, lattice and spin degrees of freedom can lead to the formation of a polaronic superlattice as observed in $La_{1.5}Sr_{0.5}NiO_4$. Figure 5 displays the behavior of $t_{\rm eff}$ (a), Δ (b), and ρ [inset (b)], as function of EP coupling for different phonon frequencies. In the adiabatic regime, we found a sequence of transitions, as ε_p increases from nearly free polarons to several charge-ordered states with frozen-in, static lattice distortions. To characterize the various states in more detail, in Table III the on-site charge and spin densities on the ten-site lattice are given at $\hbar\omega=0.8$. For small values of ε_p, the holes are completely delocalized (FP), destroying the antiferromagnetic order of the background. Note that compared to the low-doping region the squeezing phenomenon is more pronounced. For larger values of ε_p, the holes self-trap on every other site as a consequence of the static displacements fields, forming a polaronic superlattice of adiabatic Holstein polarons. This crossover is signaled by a pronounced peak in the charge structure factor $S^c(\mathbf{q})$ at (π,π).[28]

To make contact with the experimental situation in the cuprates and nickelates, we note that we obtain a critical EP coupling strength $\varepsilon_p^c\sim 1.5$ (~ 2.5) at $\hbar\omega=0.1$ (0.8) for the transition from the FP metallic phase to the (π,π) ordering of self-localized hole polarons. From an analysis of the optical conductivity data for $La_{2-x}Sr_xNiO_{4+\delta}$ and $La_{2-x}Sr_xCuO_{4+\delta}$, Bi and Eklund[3] have estimated values for the polaron parameters $\zeta=1/2\varepsilon_p$ and $\eta=2\varepsilon_p/\hbar\omega$ at low doping levels ($x\le 0.2$). In the cuprates, ζ increases from 0.33 ($x=0.02$) to 1.7 ($x=0.2$), i.e., $\varepsilon_p\ll\varepsilon_p^c$, and the small polaron contribution the optical response (conductivity) is overwhelmed by the contribution from band-like carriers (FP).[3] Contrary for the nickelates, which become metallic only near $x\approx 1$, they found a nearly doping independent ratio $\zeta\sim 0.15$ ($\eta\sim 10$, i.e., $\hbar\omega=0.625$ Ref. 37), which corresponds to $\varepsilon_p\sim 3$, indicating that the polarons are small.[38] For comparison, the classical small polaron material $TiO_{2-\delta}$ has $\zeta\sim 0.12$. As can be seen from Fig. 5(a) and Table III, at $\varepsilon_p=3$, the ground state of the quarter-filled polaronic t-J model exhibits a commensurate ordering of polarons, which qualitatively agrees with the experimental findings for the nickelates.

If in our model calculation the EP coupling is further

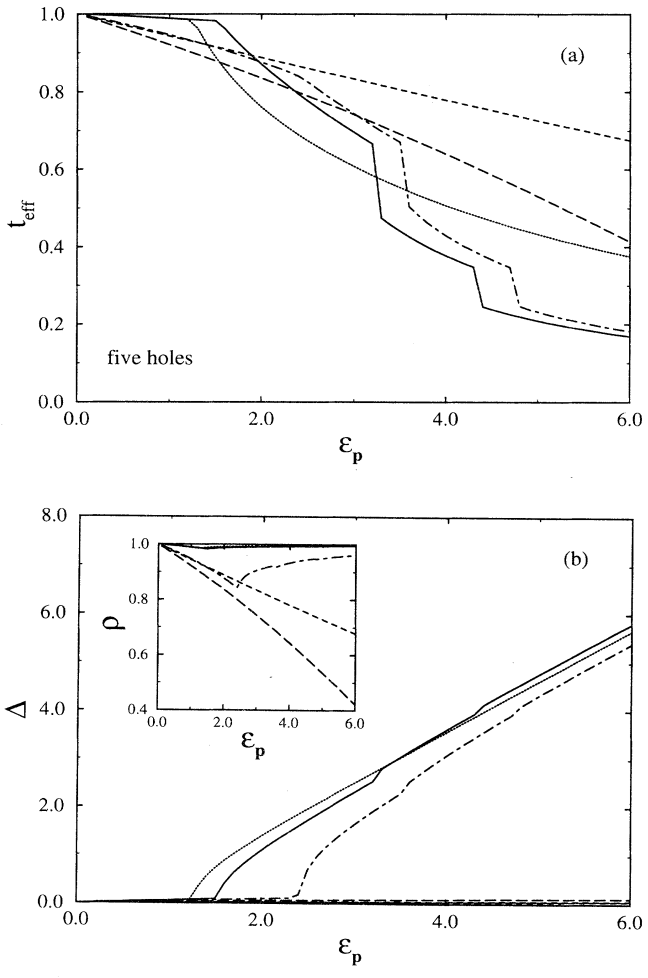

FIG. 5. $t_{\rm eff}$ (a), Δ (b), and ρ are shown as function of ε_p at quarter filling ($N_h=5$), where the solid, dotted, chain-dashed, long-dashed, and dashed curves correspond to $\hbar\omega=0.1$, 0.1 (spinless fermions), 0.8, 3.0, 10.0, respectively.

TABLE III. Ground-state energies (E), polaron/squeezing parameters (γ/τ^2), and on-site charge/spin densities ($\langle n_i\rangle/\langle S_i^z\rangle$) of the quarter-filled Holstein t-J model on a ten-site square lattice. The results are given for different EP interactions (ε_p) at $\hbar\omega=0.8$ and $J=0.4$.

ε_p	1.0	3.0	4.0	5.0
E	−12.1505	−18.6668	−22.8465	−27.4861
γ	0.219 955	0.174 848	0.120 711	0.091 083
τ^2	0.898 805	0.859 364	0.940 662	0.975 873
i		$\langle n_i\rangle/\langle S_i^z\rangle$		
1	0.5231/+0.1214	**0.1546/+0.0050**	**0.0629/+0.0098**	**0.0287/+0.0073**
2	0.5231/+0.1214	0.8451/+0.2384	0.9250/+0.1892	**0.0176/−0.0021**
3	0.5231/+0.1214	**0.1796/+0.0134**	0.9405/−0.1218	**0.0287/+0.0073**
4	**0.4654/−0.0570**	0.8451/+0.2384	**0.0599/−0.0054**	**0.0176/−0.0021**
5	**0.4654/−0.0570**	**0.1546/+0.0050**	**0.0625/+0.0118**	**0.0287/+0.0073**
6	0.5231/+0.1214	0.8083/−0.1326	0.9611/+0.3425	0.9707/+0.2698
7	0.5231/+0.1214	**0.1796/+0.0134**	0.9405/−0.1218	0.9834/−0.1636
8	0.5231/+0.1214	0.8451/+0.2384	0.9250/+0.1892	0.9707/+0.2698
9	**0.4654/−0.0570**	**0.1796/+0.0134**	**0.0625/+0.0118**	0.9834/−0.1636
10	**0.4654/−0.0570**	0.8083/−0.1326	**0.0599/−0.0054**	0.9707/+0.2698

enhanced, a second transition occurs to a striplike phase and finally, at $\varepsilon_p>4$, to a charge separated state (cf. Table III). Both transitions are accompanied by changes in the spin arrangements. In the fully phase separated state the segregation of holes becomes complete at large ε_p, where $\{\sum_i(\Delta_i^2/4\varepsilon_p)+\bar{\gamma}^2\varepsilon_p N-E_{\Delta h}\}\to 0$. At the same time, the importance of the kinetic energy part ($\propto t_{\rm eff}$) is reduced, due to the formation of self-trapped Holstein polarons. Then the physical reason for the occurrence of phase separation at *moderate* J ($J=0.4$) is that the gain in exchange energy by maximizing the number of antiferromagnetic bonds in the electron-rich part of the system may outweigh the relatively low cost in kinetic energy.

IV. COMPARING OUR VARIATIONAL LANCZOS APPROACH WITH EXACT RESULTS: HOLSTEIN-HUBBARD MODEL WITH ONE AND TWO ELECTRONS

The numerical results for the 2D Holstein t-J model discussed above are based on the IMVLF transformation (2)–(4) followed by the procedure of averaging over the transformed squeezed-phonon coherent state (5) and (6). To judge to what extent the results are reliable, we check the IMVLF method by comparison with the exact data available for the related Holstein-Hubbard model

$$\mathcal{H}_{H-H}=-t\sum_{\langle ij\rangle\sigma}(c_{i\sigma}^{\dagger}c_{j\sigma}+\text{H.c.})+U\sum_i n_{i\uparrow}n_{i\downarrow}$$
$$-\sqrt{\varepsilon_p\hbar\omega}\sum_i(b_i^{\dagger}+b_i)n_i+\hbar\omega\sum_i(b_i^{\dagger}b_i+\tfrac{1}{2})\ . \tag{18}$$

Here, the on-site *electron* occupation number $n_i=n_{i\uparrow}+n_{i\downarrow}$ is coupled to a dispersionless orbital-phonon branch. U denotes the Hubbard repulsion. We have solved the Holstein (Hubbard) model with one and two electrons on 1D rings and 2D square lattice up to ten sites, using numerical diagonalization within a truncated phononic Hilbert space. The relative error of the ground-sate energy caused by the truncation procedure was checked to be less than 10^{-8}. A detailed presentation of exact results concerning polaron and bipolaron formation in the Holstein-Hubbard model, as well as a description of the numerical procedure is given elsewhere.[14,15] Here, we only want to show that the IMVLF approach combined with Lanczos diagonalization of the effective Hamiltonian is in good agreement with the exact solution in adiabatic and nonadiabatic regimes, for a wide range of EP coupling strength. Applying the IMVLF scheme (2)–(6) with the substitution $\tilde{h}_i\to n_i$ to the Hamiltonian (18), we obtain the effective polaronic Hubbard model

$$\mathcal{H}_{H-H}^{\rm eff}=\frac{\hbar\omega}{4}N(\tau^2+\tau^{-2})+\bar{\gamma}^2\varepsilon_p N+\frac{1}{4\varepsilon_p}\sum_i\Delta_i^2+\lambda\sum_i\Delta_i$$
$$+(1-\gamma)\sum_i\Delta_i n_i-\varepsilon_p[2\gamma-\gamma^2+2\bar{\gamma}(1-\gamma)]\sum_i n_i$$
$$-\rho t\sum_{\langle ij\rangle\sigma}(c_{i\sigma}^{\dagger}c_{j\sigma}+\text{H.c.})+U_{\rm eff}\sum_i n_{i\uparrow}n_{i\downarrow}\ . \tag{19}$$

In $\mathcal{H}_{H-H}^{\rm eff}$, the bare Hubbard interaction becomes renormalized [$U\to U_{\rm eff}=U-2\varepsilon_p(2\gamma-\gamma^2)$], which raises the probability of a phonon-induced attractive interaction ($U_{\rm eff}<0$). The self-consistency equations (9)–(15), (16), and (17) can be taken over to the case of the polaronic Hubbard model (19) by using the following substitutions: $\tilde{c}_{i\sigma}^{(\dagger)}\to c_{i\sigma}^{(\dagger)}$, $\delta\to n$, $\delta_i\to\langle n_i\rangle$, and $J\to U$.

Figures 6 and 7 display the band renormalization ($\propto t_{\rm eff}$) and the ground-state energy (E) of the one-electron Holstein model in 1D and 2D, respectively. Exact results[14,15] are compared with the approximative ones as a function of EP coupling strength at two characteristic phonon frequencies, corresponding to the adiabatic

($\hbar\omega=0.4$) and nonadiabatic regimes ($\hbar\omega=3.0$). Besides the IMVLF-Lanczos method, we have used a *uniform* variational Lang-Firsov transformation[23,25] (VLF; $\Delta_i=0$) and the usual Lang-Fisov transformation (LF; $\Delta_i=0$, $\tau^2=1$, $\gamma=1$, $\bar{\gamma}=0$) to calculate $t_{\rm eff}$ and E on a ten-site cluster. As follows from the comparison, there is an overall qualitative agreement of the IMVLF-Lanczos approach with exact results in the weak- and strong-coupling cases. In particular, the IMVLF theory is able to describe the formation of the self-trapped AHP state in the adiabatic strong-coupling regime, where both LF and VLF canonical transformations are bad approximations to the true ground state. It is worthwhile to point out that the uniform LF/VLF approximations in that case give a polaronic band narrowing, which is three orders of magnitude too large $t_{\rm eff}=\rho\sim 10^{-4}$. In fact, the structure of the exact ground state deviates considerably from that of a band of extremely heavy Lang-Firsov-type polarons.[14,15] It is also interesting to note that the IMVLF-Lanczos approach reproduces to some extent the well-known differences between polaron formation in one and two dimensions. In 1D, we found a rather smooth transition from a large-size polaron to the AHP (see the discussion of Fig. 8 below). Contrary, in the 2D case the transition becomes sharp, where, of course, the nonanalytic jumplike behavior is an apparent shortcoming of the variational approach. In the nonadiabatic regime, we obtain $\Delta_i=0$, i.e., the IMVLF and VLF approaches coincide. At larger EP couplings, our variational Lanczos method, based on only two-phonon coherent states, yields too narrow a polaronic band, especially for the 1D case [see Figs. 6(b) and 7(b)]. Although the squeezing phenomena weakens the mass renormalization inherent to the polaron effect to some extent (cf. the LF results), the inclusion of higher-order phonon processes is necessary to offset the strong polaronic band narrowing more completely.

Having established the power of the IMVLF-Lanczos method, we calculate, in a next step, the phase diagram of the one-electron Holstein model in 1D and 2D. Note that the size of the clusters that this technique can reach is large enough to exclude finite-size effects. For the 2D case the transition line, presented in Fig. 8, separates two main regimes, which in the sense of Sec. III correspond to delocalized (FP) and mainly localized (AHP) states, re-

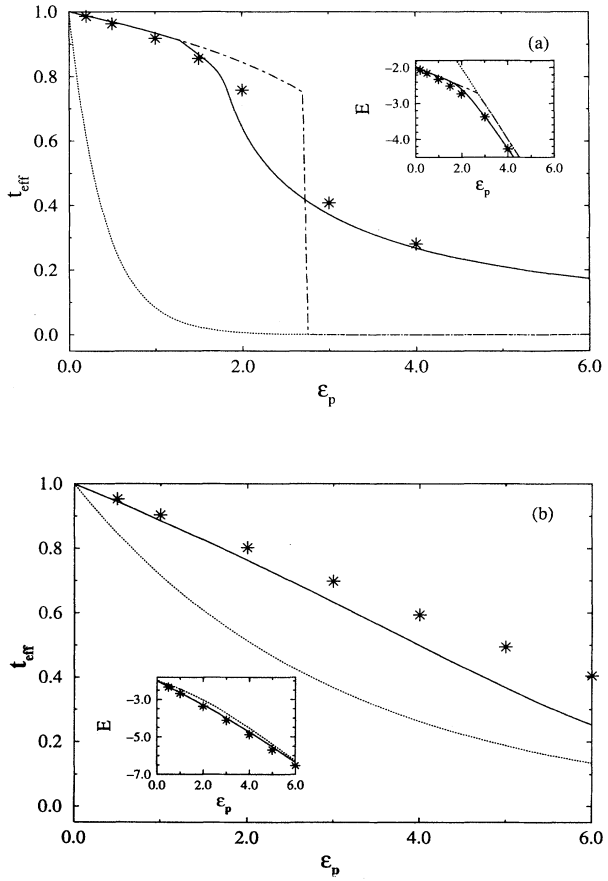

FIG. 6. Effective hopping amplitude $t_{\rm eff}$ and shifted ground-state energy $E=E_{\rm tot}-N\hbar\omega/2$ (inset), as a function of EP coupling ε_p for the 1D single-electron Holstein model at $\hbar\omega=0.4$ (a) and $\hbar\omega=3.0$ (b). Exact results for the ten-site ring (stars) are compared with approximative solutions based on the IMVLF (solid curve), VLF (chain dashed curve), and LF (dotted curve) transformations, respectively.

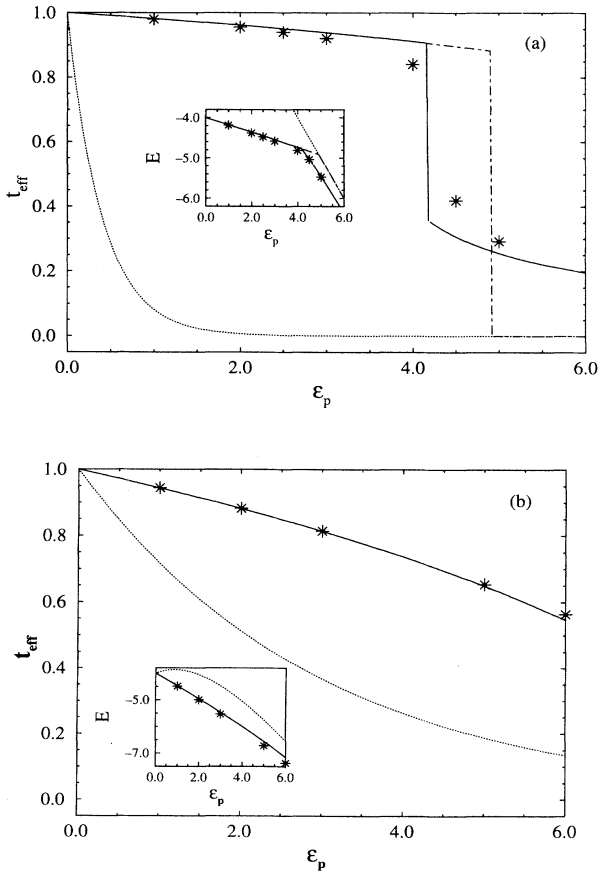

FIG. 7. $t_{\rm eff}$ and E vs ε_p for the 2D single-electron Holstein model on a ten-site square lattice at $\hbar\omega=0.4$ (a) and $\hbar\omega=3.0$ (b). The notations are the same as in Fig. 6.

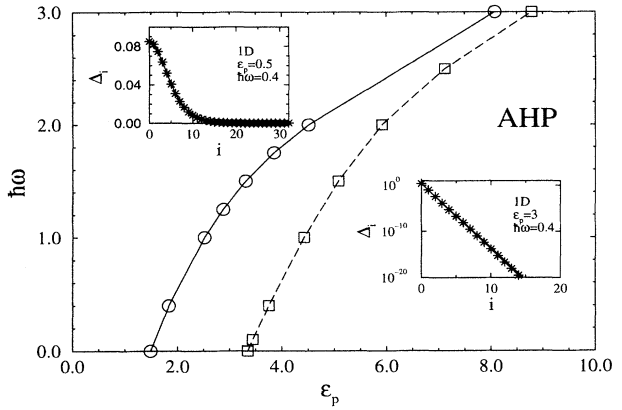

FIG. 8. Phase diagram of the 1D (2D) Holstein model with one electron, where the solid (dashed) line separates the LP (FP) state at small ε_p from the self-tapped AHP at strong EP coupling. Results are obtained for finite lattices with $N=64$ (1D, open circles) and $N=256$ (2D, open squares) sites using the IMVLF-Lanczos method. The insets show the variation of the displacement fields Δ_i away from the central site $i=0$ for two characteristic parameter values $(\varepsilon_p,\hbar\omega)$ corresponding to different types of polaronic states in the 1D case.

spectively. Within our variational treatment, the transition is of first order. In accordance with recent results,[22] we find a small metastability region just above the transition point, where the FP (metastable) state is separated by an energy barrier from the AHP state. In the 1D case, the results differ from the 2D case essentially. Performing a finite-size analysis, it can be shown[14,15] that the FP state becomes unstable at any finite EP coupling. Instead we observe a large-size polaron in the weak-coupling regime, which continuously turns into a small-size polaron with increasing EP coupling. In this case, we identified the critical a value of EP coupling with the minimum in the second derivative of the total energy with respect to ε_p. For $\varepsilon_p<\varepsilon_p^c$, the polaron density grows with increasing ε_p for several sites around the center of the polaron, whereas for $\varepsilon_p>\varepsilon_p^c$, the polaron density becomes enhanced at the central site $i=0$ only as ε_p increases. To elucidate in 1D the different nature of self-trapped polaronic states occurring in the adiabatic strong and weak EP coupling regimes, we present in the insets of Fig. 8 the variation of the displacement fields away from the central site $i=0$ (where, the polaron is assumed to be located). For the large-size polaron, the lattice displacements fits extremely well to the functional form,

$$\Delta_i=a_0\,\mathrm{sech}^2(a_1 i) \tag{20}$$

[cf. the solid curve in Fig. 8 (upper inset)], where $(2a_1)^{-1}$ defines the polaron radius and the distances i are measured in units of the lattice constant a. It should be emphasized that the result (20) was derived more recently within an alternative approach to polaron formation in 1D based on the solution of a nonlinear Schrödinger equation.[39] In contrast, we obtain for the AHP an exponential decay of the lattice distortions,

$$\Delta_i=\Delta_0 e^{-i/\xi}\,, \tag{21}$$

away from the polaron site [see Fig. 8 (lower inset)]. Here, ξ denotes the radius of the small-size polaron. We found $\xi\sim 0.3$, i.e., for large ε_p the self-trapped AHP is confined to a single lattice site.

Finally, we consider the 1D Holstein-Hubbard model with two electrons. The most noteworthy aspect of this problem is the question of bipolaron formation, which will be discussed in more detail in a forthcoming paper.[15] Here, we would like to point out that the main effects of the two-electron problem (e.g., the tendency to bipolaron formation) can be described even quantitatively within our IMVLF scheme. The comparison of the IMVLF results with the exact data for ground-state energy and t_{eff} is presented in Fig. 9 in the adiabatic [$\hbar\omega=0.4$ (a)] and nonadiabatic [$\hbar\omega=3.0$ (b)] regimes at $U=6$. Obviously, the IMVLF method gives a satisfactory estimate for both E and the polaronic bandwith in a wide coupling region. In the adiabatic case, we can distinguish three different regimes. For low ε_p, the ground state resembles that of two quasifree polarons. The nearly-free polaron state is stabilized by the intramolecular Coulomb repulsion and, in 1D, does not exist for $U=0$.[11,14] As ε_p exceeds a criti-

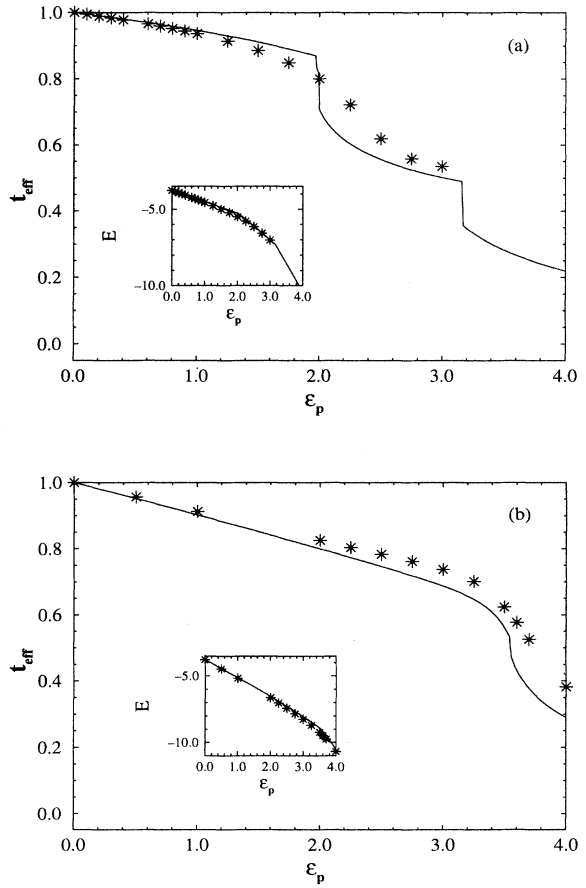

FIG. 9. Effective hopping amplitude t_{eff} and ground-state energy E (inset) as a function of EP coupling ε_p for the 1D Holstein-Hubbard model with two electrons. For $U=6$, exact results for the eight-site lattice with 20 phonons (stars) are compared with IMVLF-Lanczos approach (solid curve) at $\hbar\omega=0.4$ (a) and $\hbar\omega=3.0$ (b).

cal value [$\varepsilon_{c,1}(U) \sim 1.2$ for our choice of parameters], the binding energy of two electrons becomes negative and at $\varepsilon_p \sim 2$ a transition to an extended bipolaronic state takes place. Here, the density-density correlation $\langle n_{0,\uparrow} n_{0+l,\downarrow} \rangle$ exhibits a maximum for $l=1$, i.e., on neighboring sites. When U_{eff} becomes negative, the electron pair is tightly bound on the same site forming an on-site bipolaron. In fact, we found for $\varepsilon_p = 3.5$ a large negative binding energy $E_B^2 = -0.916$. At the same time, the local magnetic moment [$\propto \langle (n_{0,\uparrow} - n_{0,\downarrow})^2 \rangle$] decreases dramatically, giving further evidence for the formation of an on-site bipolaron. Increasing the phonon frequency, the intermediate intersite bipolaronic state is smeared out and the crossover to the onset bipolaron is shifted to large values of the EP coupling [cf. Fig. 9(b)].

V. SUMMARY

In this paper, we have performed an extensive numerical study of the 2D Holstein t-J model on finite square lattices in order to investigate the problem of hole-polaron formation in strongly correlated electron-phonon systems. On the basis of an IMVLF, we propose a variational Lanczos approach for the effective polaronic t-J model that allows for the description of static displacement field, polaron, and squeezing effects, and contains the strong Coulomb correlations in an exact way. The method is designed to investigate the interplay between electron-electron and EP interactions at arbitrary band fillings for a wide range of phonon frequencies, where both adiabatic and antiadiabatic limiting cases are well reproduced. The finite-size effects in the results were checked to be small.

The quality of the IMVLF approach was demonstrated by comparison with exact diagonalization results available for the 1D Holstein-Hubbard model with one and two electrons. In this case, the IMVLF-Lanczos method describes the qualitative features of the model and provides an excellent estimate for ground-state energy and polaronic band renormalization.

Concerning the ground-state properties of the polaronic t-J model in the one- and two-hole sector, our main results are the following.

(i) In the adiabatic regime, we find a *narrow* crossover region from nearly FP to AHP, as the EP coupling (ε_p) increases. This transition is accompanied by a strong renormalization of the polaronic bandwidth ($\propto t_{\text{eff}} \neq \rho$) and the occurrence of an *inhomogeneous* displacement field. Whereas the "delocalized" FP state reflects the translation symmetry of the ground state of the pure t-J model, the AHP becomes quasilocalized (self-trapped), due to a strong *local* lattice distortion. In the nonadiabatic regime, we found a *smooth* evolution from FP to Lang-Firsov-type polarons (NLFP). The NLFP state is characterized by a rather *moderate* polaronic mass enhancement and a *uniform* distribution of the static displacement fields. Note that an extremely heavy NLFP ($t_{\text{eff}} = \rho \to 0$) does *not* exist.

(ii) The critical EP coupling strength for the self-trapping transition of the doped charge carriers is considerably reduced by the antiferromagnetic exchange interaction compared to that in the uncorrelated model (spinless fermions). This means that a rather weak EP interaction can cause polaronic band narrowing in strongly correlated electron systems supporting a prominent role of the lattice degree of freedom in the cuprates and even more in the isostructural nickelates.

(iii) The finite density (many-polaron) effects on the hole-polaron formation, treated by the IMVLF-Lanczos approach, are mainly realized via correlation and squeezing effects, which counteract each other and become most pronounced in the low- and high-doping regime, respectively. Therefore, with increasing hole density, the transition to the AHP state is shifted to higher EP couplings.

(iv) Analyzing the two-hole binding energy in the 2D polaronic t-J model, we have found that hole binding is enhanced in the weak-coupling (FP) regime as a dynamical effect of the EP interaction. In this case, the strongest attraction of hole polarons results for intermediate phonon frequencies, being comparable in magnitude to the renormalized transfer amplitude. On the other hand, in the strong EP coupling (adiabatic) case, a static type of hole binding is realized, where the two holes become self-trapped on nearest-neighbor sites forming a nearly immobile bipolaron.

For the quarter-filled band case, the ground-state of the polaronic t-J model exhibits a sequence of transitions as the EP coupling increases from a FP state to a polaronic superlattice related to a frozen-in (π,π) lattice distortion and finally to a phase (charge) separated state. Let us emphasize that the experimental estimates of the polaron parameters (ξ,η) for the cuprates and nickelates coincide with the values where we find the FP and the commensurate polaronic superlattice in the Holstein t-J model.

ACKNOWLEDGMENTS

We would like to thank D. Ihle for useful discussions. This work was supported in part by the European Economic Community under Contract No. SC1*-CT91-0686.

[1] H. Rietschel, J. Low Temp. Phys. **95**, 293 (1994).
[2] J. Zhong and H.-B. Schüttler, Phys. Rev. Lett. **92**, 1600 (1992).
[3] X. X. Bi and P. C. Eklund, Phys. Rev. Lett. **70**, 2625 (1993).
[4] *Lattice Effects in High-T_c Superconductors,* edited by Y. Bar-Yam, T. Egami, J. Mustre-de Leon, and A. R. Bishop (World Scientific, Singapore, 1992), pp. 377–422, and references therein.
[5] I. Poberraj and D. Mihailovic, Phys. Rev. B **50**, 6426 (1994).
[6] L. D. Landau, Z. Phys. **3**, 664 (1933).
[7] B. Gerlach and H. Löwen, Rev. Mod. Phys. **63**, 63 (1991).
[8] A. S. Aleksandrov and A. B. Krebs, Usp. Fiz. Nauk **162**, 1 (1992) [Sov. Phys. Ups. **35**, 345 (1992)].

[9]A. L. Shluger and A. M. Stoneham, J. Phys. Condens. Matter **5**, 3049 (1993).
[10]A. S. Aleksandrov and N. F. Mott, Int. J. Mod. Phys. B **8**, 2075 (1994); Rep. Prog. Phys. **57**, 1197 (1994).
[11]J. Ranninger and U. Thibblin, Phys. Rev. B **45**, 7730 (1992).
[12]F. Marsiglio, Phys. Lett. A **180**, 280 (1993).
[13]A. S. Aleksandrov, V. V. Kabanov, and D. K. Ray, Phys. Rev. B **49**, 9915 (1994).
[14]G. Wellein, Diploma thesis, University of Bayreth, 1994.
[15]G. Wellein, H. Röder, and H. Fehske (unpublished).
[16]A. N. Das, J. Konior, and D. K. Ray, Physica C **170**, 215 (1990).
[17]D. Feinberg, S. Ciuchi, and F. de Pasquale, Int. J. Mod. Phys. B **7&8**, 1317 (1990).
[18]F. Marsiglio (unpublished).
[19]H. D. de Raedt and A. Lagendijk, Phys. Rev. B **27**, 6097 (1983).
[20]I. G. Lang and Y. A. Firsov, Zh. Eksp. Teor. Fiz. **43**, 1843 (1962) [Sov. Phys. JETP **16**, 1301 (1963)].
[21]T. Holstein, Ann. Phys. **8**, 325 (1959); **8**, 343 (1959).
[22]V. V. Kabanov and O. Y. Mashtakov, Phys. Rev. B **47**, 6060 (1993).
[23]H. Zheng, D. Feinberg, and M. Avignon, Phys. Rev. B **39**, 9405 (1989).
[24]A. Muramatsu and W. Hanke, Physica C **153-155**, 229 (1988).
[25]H. Zheng, Phys. Rev. B **37**, 7419 (1988).
[26]H. Fehske, D. Ihle, J. Loos, U. Trapper, and H. Büttner, Z. Phys. B **94**, 91 (1994); U. Trappr, H. Fehske, M. Deeg, and H. Büttner, *ibid.* **93**, 465 (1994).
[27]H. Fehske, H. Röder, A. Mistriotis, and H. Büttner, J. Phys. Condens. Matter **5**, 3565 (1993).
[28]H. Röder, H. Fehske, and R. N. Silver, Europhys. Lett. **28**, 257 (1994).
[29]For a review on numerical work on the t-J model, see E. Dagotto, Rev. Mod. Phys. **66**, 763 (1994).
[30]Classification of the one-hole ground state of the t-J model on a ten-site square lattice: $\mathbf{k}=(0,0)$, $S=\frac{1}{2}[J\geq 3.39]$; $\mathbf{k}$ is one out of the star of $\mathbf{k}=(3\pi/5,\pi/5)$, $S=\frac{1}{2}[3.39\geq J\geq 0.262]$; $\mathbf{k}$ is one out of the star of $\mathbf{k}=(2\pi/5,4\pi/5)$, $S=\frac{1}{2}[0.262\geq J\geq 0.184]$; $\mathbf{k}=(\pi,\pi)$, $S=\frac{3}{2}[0.814\geq J\geq 0.147]$; $\mathbf{k}=(0,0)$, $S=\frac{5}{2}[0.184\geq J\geq 0.138]$; and $\mathbf{k}=(0,0)$, $S=9/2$ for J less than the Nagaoka value $J(N=10)=0.138$.
[31]C. H. Chen, S.-W. Cheong, and A. S. Cooper, Phys. Rev. Lett. **71**, 2461 (1993); S. W. Cheong *et al.*, Phys. Rev. B **49**, 7088 (1994).
[32]V. I. Anisimov, M. A. Korotin, J. Zaanen, and O. K. Andersson, Phys. Rev. Lett. **68**, 345 (1992).
[33]S. M. Hayden *et al.*, Phys. Rev. Lett. **68**, 1061 (1992).
[34]E. D. Isaacs *et al.*, Phys. Rev. Lett. **72**, 3421 (1994).
[35]J. Zaanen and P. B. Littlewood, Phys. Rev. B **50**, 7222 (1994).
[36]A. M. Oleś, L. F. Feiner, and J. Zaanen (unpublished).
[37]L. Pintschovious *et al.*, Phys. Rev. B **40**, 2229 (1989).
[38]H. G. Reik, Z. Phys. **203**, 346 (1967).
[39]A. H. Castro Neto and A. O. Caldeira, Phys. Rev. B **46**, 8858 (1992).